AXAA

Australian X-ray Analytical Association

Newsletter Issue 2 2022

President's Address

Hello AXAA Members and Friends,

I would like to use this opportunity to generate interest in AXAA's upcoming *in person* seminars in various states.

Many of us have fond memories of the AXAA student seminar days, but this time we will be opening up to all AXAA members and friends and strengthening the social offering. It's been a long time since we've been able to come together in person, so we hope to provide local opportunities for networking over a meal, with quality talks from AXAA members both junior and senior. Keep an eye out for our emails about sponsorship opportunities and presentation callouts in your state!

Secondly, we are seeking your input for a new database of X-ray analytical facilities in Australia which will be hosted on the AXAA website. Please take note of the Community News item below, we are looking for feedback on how we can best serve the community and would love to hear from you.

XAFS2022 Conference wrap-up

Recently I attended the international XAFS2022 conference which was held at Sydney University in July. Preceding the conference, we held a symposium at the Australian Synchrotron with invited talks on beamline upgrades and scientific applications from as far away as Brazil and the UK. A major focus of the day was tender XAS, and the capabilities of the currently-commissioning Medium Energy XAS (MEX) beamlines at the Australian Synchrotron. Tours allowed participants on-site to get a close-up look at the new equipment and chat to beamline scientists about potential experiments.

The conference in Sydney kicked off with an excellent workshop on Larch, a python-based XAS data analysis software by Matt Newville (University of Chicago), and was then followed by 5 days of science talks! Particular highlights for me were keynote presentations by Sofia Diaz-Moreno on state-of-the-art upgrades to the spectroscopy suite of beamlines at Diamond, and Wantana Klysubun (Synchrotron Light Research Institute, Thailand) on how X-ray methods can help differentiate fake from genuine historical artefacts.

Uwe Bergmann (University of Wisconsin-Madison) gave a fascinating public lecture in University of Sydney's Chau Chak Wing Museum. We saw how high resolution XRF revealed ancient scripts written by Archimedes, that had been destroyed and written over in later centuries. The same techniques have also been applied to fossils, for example in differentiating light and dark pigments in dinosaur feathers.

Finally, we celebrated the iXAS awards, including the Edward Stern Outstanding Achievement Award to both Matt Newville (U. Chicago) and Bruce Ravel (NIST) for their lifetime of dedication and efforts in providing software tools and training for the XAS community around the world. Anyone who has used XAS will appreciate the useability of the free software Athena and Larch, and the abundance of online video training resources, as well as the in-person workshops both Matt and Bruce provide. They really have enabled countless scientists to use XAS through a solid foundation of data processing know-how.

Jessica Hamilton
AXAA President

AXAA is compiling an Australian X-ray facility database

In the coming months AXAA will be compiling a list of X-ray facilities around Australia. The intent is to connect users with the techniques they need, as well as to help facilities advertise their capabilities with researchers across academia and industry. We will be collecting information about capabili-

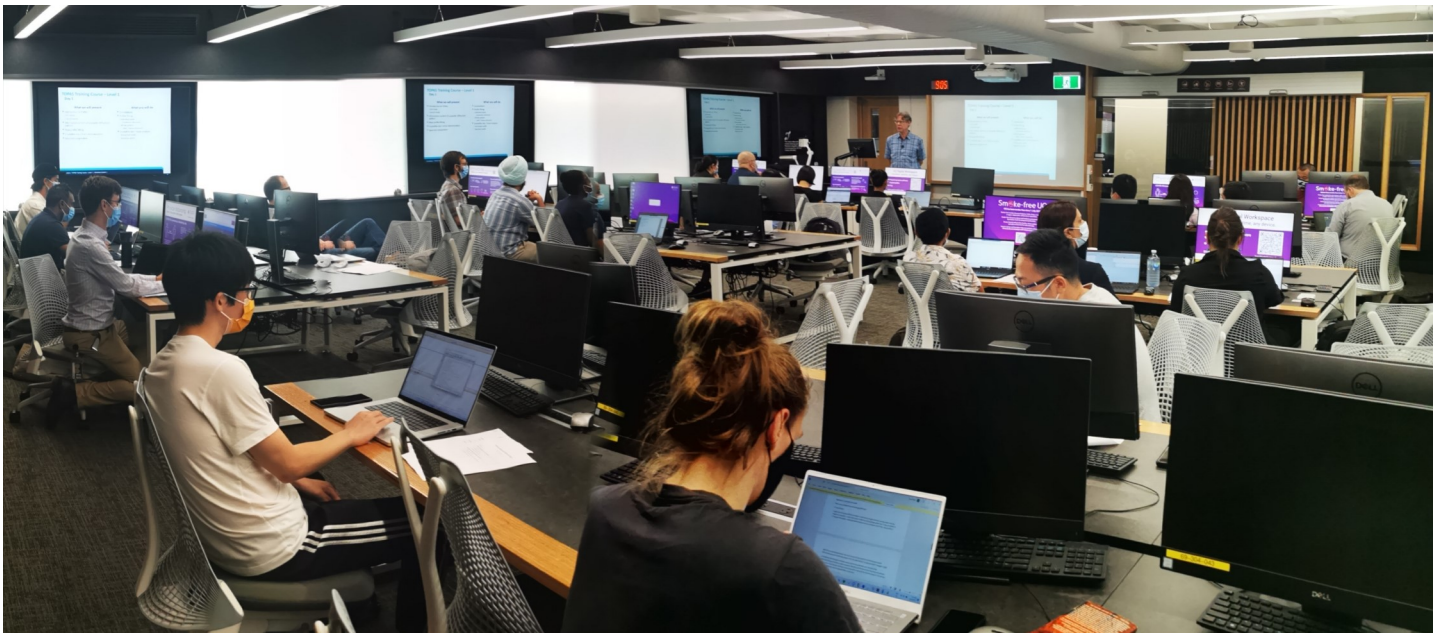

Ian Madsen guides attendees through XRD analysis at UQ-QUT's TOPAS workshop

ties around various X-ray techniques including XRD, SAXS, XPS, XRF, and X-ray CT as well as complimentary techniques and sample preparation facilities. We would like to invite anyone in the AXAA community to reach out to us at ausxray@gmail.com with any suggestions or feedback, or if they would like to see their facility included.

UQ-QUT 3 day TOPAS workshop

Education for the next generation X-ray Diffraction practitioners

Dr. Tony Wang
Research Infrastructure Specialist
CARF, QUT

AXAA life member Ian Madsen was invited to give a 3-day TOPAS WORKSHOP to young researchers in the University of Queensland and Queensland University of Technology between 20th to 22nd April 2022. In the first two days, the workshop guided the audience through TOPAS GUI functionalities including convolution based peak profile fitting, instrument broadening parametrization, sample micro-structure analysis, quantitative phase analysis, and Rietveld crystal structure refinement. Other commonly overlooked issues preventing accurate quantification including sample preparation, micro-absorption, space group settings from different databases etc. were also discussed. On the third day, the audience were guided as they explored the coding operations in jEdit and the flexibility of using TOPAS launch mode for batch refinement of in-situ XRD data. After the workshop, Ian was invited to visit the X-ray Lab in Centre for Microscopy and Microanalysis, University of Queensland and the X-ray Lab in Central Analytical Research Facility, Queensland University of Technology. The workshop was co-organized by Bruker Pty. Ltd.

CSIRO Team Places Second in 2022 Reynolds Cup Competition

A CSIRO team consisting of Mark Raven, Rong Fan, Rodrigo Gomez-Camacho, Peter Self, Nick Owen, Shu Huang and Nathan Webster has achieved second place in the 2022 Reynolds Cup Competition. The biennial global competition is for accuracy in quantitative mineral analysis, with emphasis on clay mineralogy, with three samples containing mineral mixtures commonly found in clay bearing rocks or soils to be analysed by each participating laboratory in a blind round robin format. This

affords participants an opportunity to test their methods in sample preparation, data collection and analysis and thereby identify both strengths and weaknesses and how they may improve. Mark and Peter are previous winners of the competition, in 2010, and the team also achieved second place in 2016 and 2020.

The CSIRO team: from left to right, Peter Self, Rodrigo Gomez– Camacho, Mark Raven, Rong Fan. Inset, Nathan Webster and Shu Huang. Absent, Nick Owen

The team analysed samples by X-ray diffraction and X-ray fluorescence after careful and rigorous preparation, with the XRD data analysed using TOPAS software and complemented with NEWMOD2. Each sample presented its own distinct challenges, such as quantification of illite/smectite interstratified clay in two of the three samples, and the presence of various aluminosilicates such as halloysite, kaolinite, dickite and nacrite across two of the three samples.

The team's achievement was announced at the recent 17th AIPEA - International Clay Conference (July 25-29, 2022 in Istanbul, Turkey).

On the sharing and visualisation of powder diffraction data.

Matthew Rowles
Technical Specialist (Mineralogy), Intertek
Adjunct Research Fellow, Curtin University

The Crystallographic Information Framework (CIF) (Bernstein *et al.*, 2016, Hall *et al.*, 1991, Hall & McMahon, 2005) is a human- and machine-readable text-based file format for the exchange of crystallographic information. Originally constructed for single-crystal data, the core CIF dictionary has been extended to include topics such as restraints, modulated structures, magnetic structures, topology, and powder diffraction data (Toby, 2006b, a) – pdCIF – amongst others. All current CIF dictionary definitions are available from the International Union of Crystallography (IUCr) (2021a).

CIF files are useful for transferring crystallographic data between different software packages, instruments, users, or institutions in a way that enables other software packages, instruments, users, or institutions to read, use, or store that information. The data is presented in a machine-readable fashion, allowing the next user or program to (hopefully) read it and carry on with an analysis or report; you don't (necessarily) require access to the same program which created the file in the first place in order to visualise data or structures. Taking this to an extreme, some crystallographic journals reporting crystal structures require their journal articles to be submitted in CIF format, with the final paper constructed from the metadata enclosed in that file.

The collection of dictionaries that make up the CIF standard, as well as the standard itself, is maintained by the IUCr Committee for the Maintenance of the CIF Standard (COMCIFS). COMCIFS maintains and establishes policy around the CIF, receives and examines proposals to extend or create dictionaries, and maintains CIF documentation, among other duties. Membership of the committee is world-wide, and it is currently

chaired by Dr James Hester (ANSTO).

pdCIF (Toby, 2006b, a) comprises a set of data items for the description of powder diffraction data, extending the original CIF implementation to include documenting instrumental conditions, as well as the powder diffraction data itself. pdCIF allows for the linking of structures to specific diffraction data, as well as diffraction data to other diffraction data, allowing for the description of complicated experiments using X-ray or neutron diffraction from the laboratory or national facilities. Moreover, it provides an agnostic way to save and share diffraction data, eschewing proprietary binary formats, or deeply nested XML tables, allowing easy reuse of data.

This last application falls under the banner of FAIR data: that data should be Findable, Accessible, Interoperable, and Reusable (Wilkinson *et al.*, 2016, ARDC, 2022). CIF provides an accepted vocabulary for describing the data and metadata that enhances discoverability, particularly through the use of machines for finding and using data. Research institutions and funding bodies, including the ARC and NHMRC, are increasingly encouraging the publication of research data, and following the FAIR principles can maximise the impact that data will provide.

There are a variety of tools available for the creation, viewing, and editing of CIF files, many of which are listed online (IUCr, 2021b). When submitting manuscripts to IUCr journals, the most important of these are checkCIF and publCIF, for CIF validation and paper preparation, respectively. However, there is a dearth of end-user tools that work well with pdCIF, and as a result, the adoption of pdCIF is not as widespread as it should be. Common powder diffraction analysis software packages are often capable of outputting diffraction data and model results, most often Rietveld refinements (Loopstra & Rietveld, 1969, Rietveld, 1969), in pdCIF format, but are then not able to read in those same files. This lack of interoperability makes studying the data and models by a third-party a difficult process without access to the original software and analysis files. One previous software package, *pdCIFplot* (Toby, 2003) was written to perform this task, but is no longer maintained. The IUCr maintain an online tool, *plotCIF* (IUCr, 2021c), which provides largely the same capability. Both are limited to showing a single diffraction pattern at a time.

I have tried to help address some of these issues through writing a series of macros (Rowles, 2022a) for TOPAS (Coelho, 2018), as well as writing a pdCIF visualisation program, *pdCIFplotter* (Rowles, 2022b), for inspecting the diffraction data contained within a pdCIF file[1]. The use of the TOPAS macros simplifies and automates many of the processes necessary to produce a valid pdCIF file containing crystal structures, raw data, and a refined model. There are several pre-defined parameter names, which trigger the inclusion of the correct data items in the pdCIF. Crystal structures and diffraction data are automatically linked, and metadata such as temperature, pressure, and a collection date/time, can be easily included. Refinements with single or many crystal structures, and/or single or many diffraction patterns are supported.

pdCIFplotter allows users to inspect diffraction data, and any refined model, saved in pdCIF format. The key concept on visualising data with *pdCIFplotter* is that all diffraction patterns that are related by some key feature should be contained in a single CIF file. For example, in an in situ experiment, powder diffraction data are included in the CIF in the order in which they were collected, with all information about temperature, pressure, collection time, as well as the calculated patterns, R factors (Toby, 2006c), and refined crystal structures as a result of any Rietveld modelling.

To allow flexibility in visualisation, there are three built-in plot types: single, stack, and surface. The single plot is designed for visualising a single diffraction pattern at a time, most often in conjunction with the results of a Rietveld model – see Figure 1. Stack plots are used to display multiple diffraction patterns where each pattern is vertically offset from the others – see Figure 2. Surface plots show a top-down view of series of diffraction patterns where the intensity of each point is represented by a colour – see Figure 3. The data

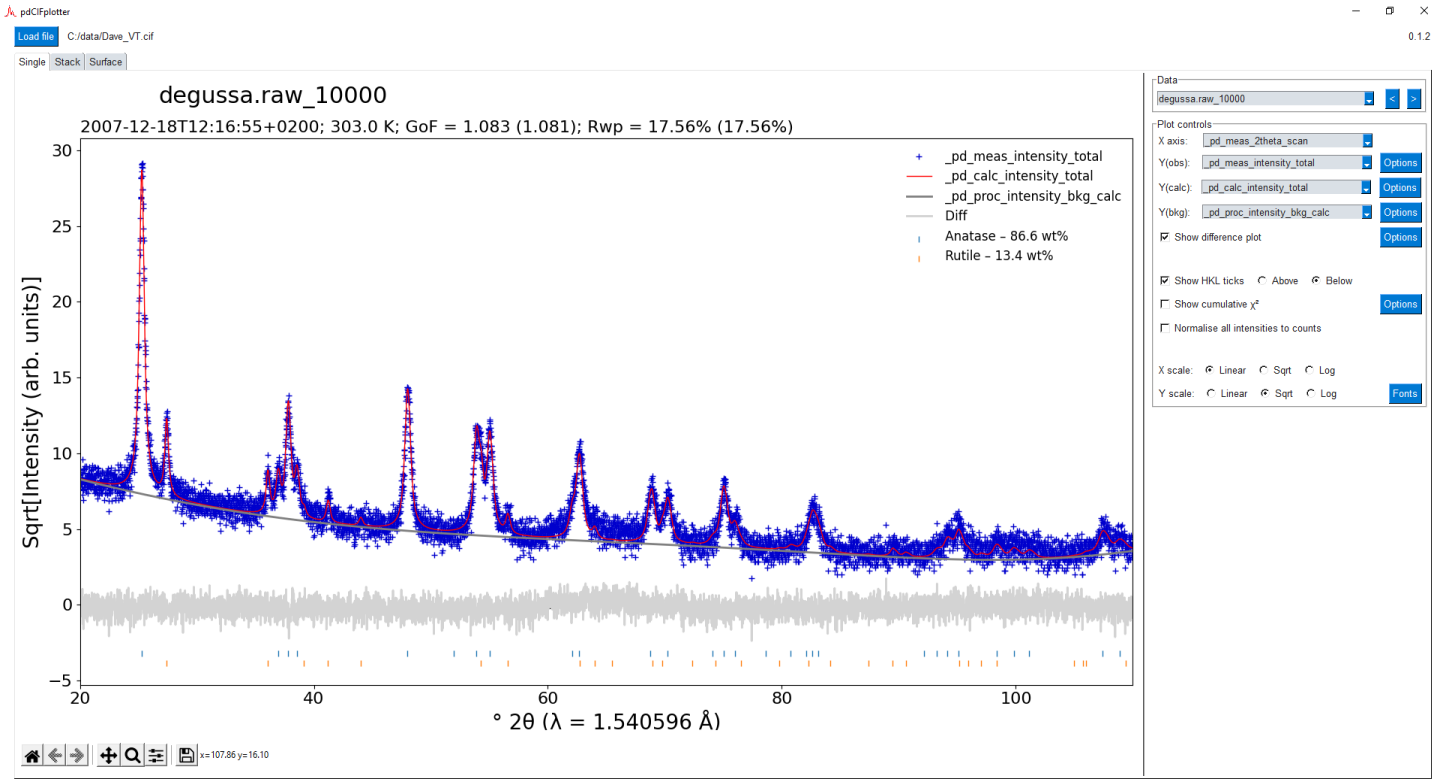

Fig 1. An example of a single diffraction pattern plot. The plot title is the block id. The subtitle summarises the date/time, temperature, pressure, goodness-of-fit, and R_{wp} values, if given. If it is possible, the GoF and R_{wp} values are calculated and given in brackets. Quantitative phase results are displayed for each phase if given. Information about each HKL tick mark is given by hover text. Example data taken from Billing (2021).

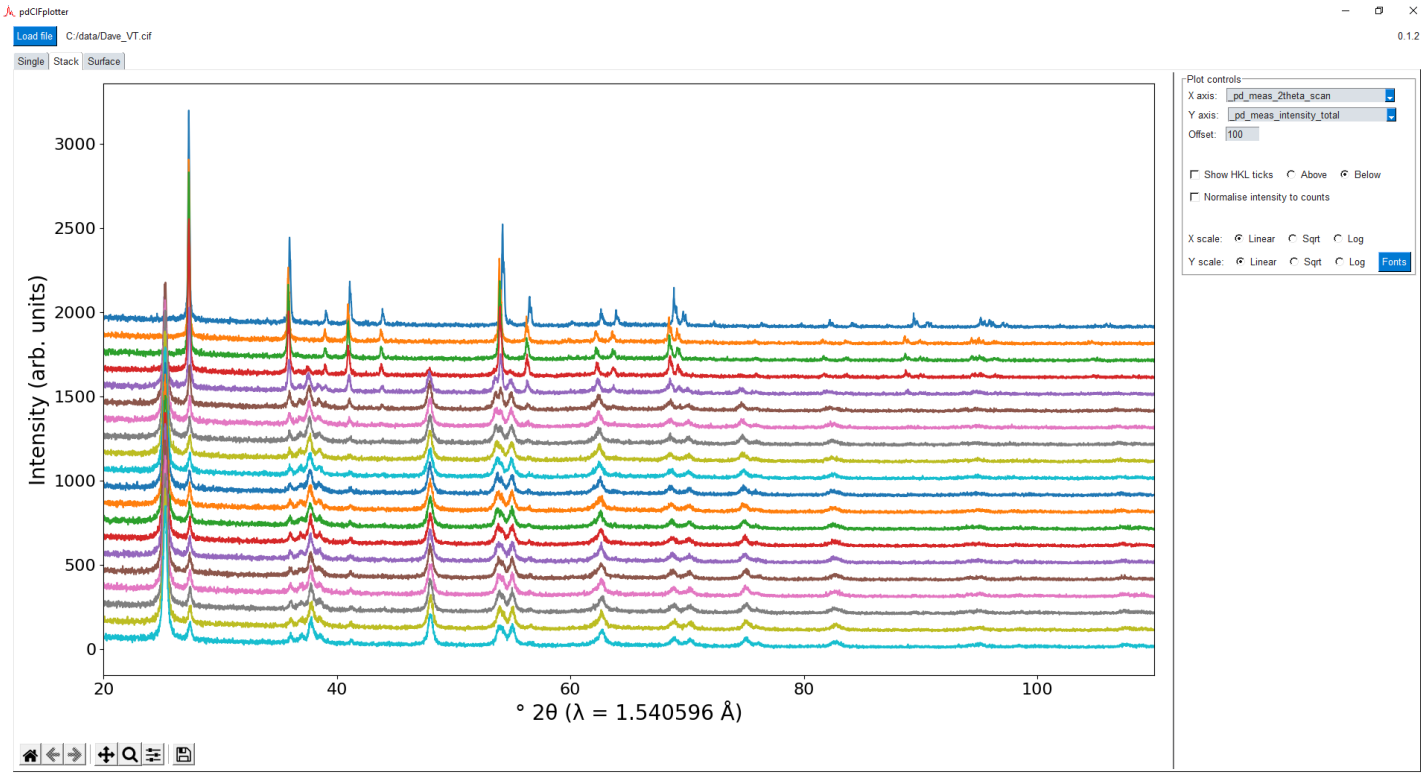

Fig 2. Example of a stack plot. Hover text for each diffraction pattern displays the block id, date/time, temperature, pressure, goodness-of-fit, and R_{wp} values, if given. Example data taken from Billing (2021).

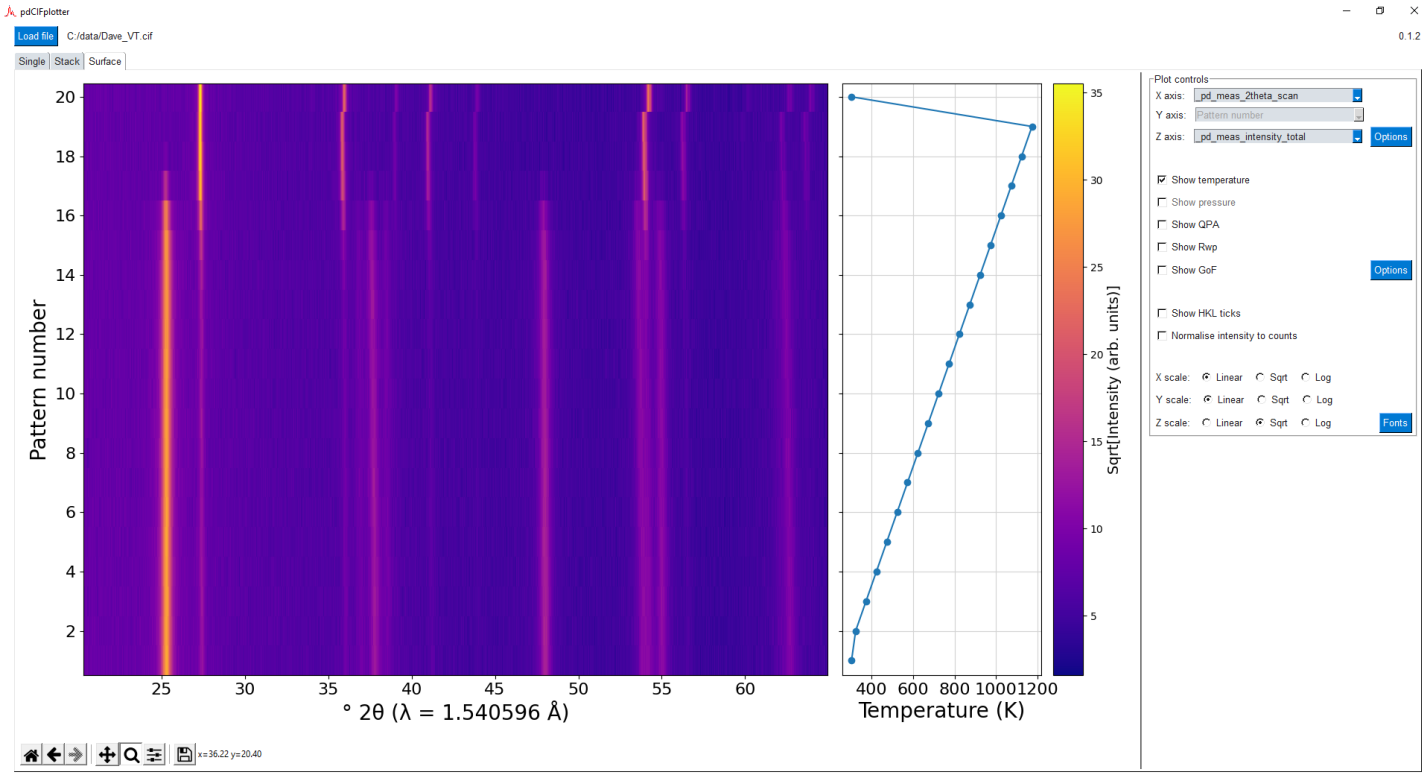

Fig 3. Example of a surface plot with the optional plot showing the temperature at which the diffraction data were collected. The y-axis is common between the two plots. Example data taken from Billing (2021).

pdCIFplotter is written in Python 3 and is available for download and installation from github[2] and PyPI[3]. The program is made available under the Apache 2.0 licence. For ease of use, *pdCIFplotter* can be downloaded as a zip file containing all necessary Windows files.[4]

The use of CIF, and pdCIF in particular, in the powder diffraction community is predicated on the ability to make use of the files that we make. Its growth hinges on software and instrumentation supporting the format and diffractionists using it. While this is a bit of a "chicken and egg" argument, CIF is a long-standing data format that is mature and under current development, meaning that it can grow with the community. Hopefully my efforts are of use to some people, and help spur the development of more software in this area, allowing for greater leverage of the data we produce.

Some more links available at:

[1] https://www.iucr.org/resources/commissions/powder-diffraction/projects/pdcif

[2] https://github.com/rowlesmr/pdCIFplotter

[3] https://pypi.org/project/pdCIFplotter/

[4] https://www.iucr.org/__data/iucr/powder/pdcif_apps/pdCIFplotter.zip

References

ARDC (2022). *FAIR Data,* https://ardc.edu.au/resources/aboutdata/fair-data/.

Bernstein, H. J., Bollinger, J. C., Brown, I. D., Gražulis, S., Hester, J. R., McMahon, B., Spadaccini, N., Westbrook, J. D. & Westrip, S. P. (2016). *J. Appl. Crystallogr.* **49**, 277-284.

Billing, D. G. (2021). Private communication.

Coelho, A. A. (2018). *J. Appl. Crystallogr.* **51**, 210-218.

Hall, S. R., Allen, F. H. & Brown, I. D. (1991). *Acta Crystallogr. A* **47**, 655-685.

Hall, S. R. & McMahon, B. (2005). Editor. *International Tables for Crystallography*, Dordrecht, The Netherlands: Springer.
IUCr (2021a). *CIF Dictionaries,* https://www.iucr.org/resources/cif/dictionaries.
IUCr (2021b). *Software for CIF and STAR,* https://www.iucr.org/resources/cif/software.
IUCr (2021c). *plotCIF,* https://publcif.iucr.org/services/tools/pdcifplot.php.
Loopstra, B. O. & Rietveld, H. M. (1969). *Acta Crystallogr. B* **25**, 787-791.
Rietveld, H. M. (1969). *J. Appl. Crystallogr.* **2**, 65-71.
Rowles, M. R. (2022a). *Powder CIF Output,* http://topas.dur.ac.uk/topaswiki/doku.php?id=out_pdcif.
Rowles, M. R. (2022b). *J. Appl. Crystallogr.* **55**, 631-637.
Toby, B. H. (2003). *J. Appl. Crystallogr.* **36**, 1285-1287.
Toby, B. H. (2006a). *International Tables for Crystallography Volume G: Definition and Exchange of Crystallographic Data,* edited by S. R. Hall & B. McMahon, pp. 117-130.
Toby, B. H. (2006b). *International Tables for Crystallography Volume G: Definition and Exchange of Crystallographic Data,* edited by S. R. Hall & B. McMahon, pp. 258-269.
Toby, B. H. (2006c). *Powder Diffr.* **21**, 67-70.
Wilkinson, M. D., *et al* (2016). *Sci Data* **3**, 160018.

Tuning the water content of iron fluoride

Olga Narygina[a], Gwilherm Nénert [b], Kerstin Forsberg [c]

[a]*Malvern Panalytical, a division of Spectris Australia Pty Ltd., Sydney, NSW, Australia;*
[b]*Malvern Panalytical B.V., Almelo, the Netherlands;*
[c]*School of Chemical Science and Engineering, Royal Institute of Technology, Stockholm, Sweden*
ON: olga.narygina@panalytical.com

Introduction

Iron fluoride (b-$FeF_3.nH_2O$) is a promising cathode material, electrochemical performance of which is strongly dependent on the rate of hydration[1-3]. b-$FeF_3.nH_2O$ is formed by infinite chains of corner-sharing $FeF_4(H_2O)_2$ octahedra held by hydrogen-bonds from water molecules (Figure 1). Hereafter we refer to this water as "structural water". Water molecules, occupying the interstitial space, the space in between the Fe-octahedra chains, we will denote as "crystalline water". Unlike structural water crystalline water is weakly bonded to the network. Its removal would create a network of one-dimensional channels with ~ 2.9 Å in diameter. These channels can be filled by small ions, e.g. lithium. The capacity for lithium intercalation in the structure would be inversely related

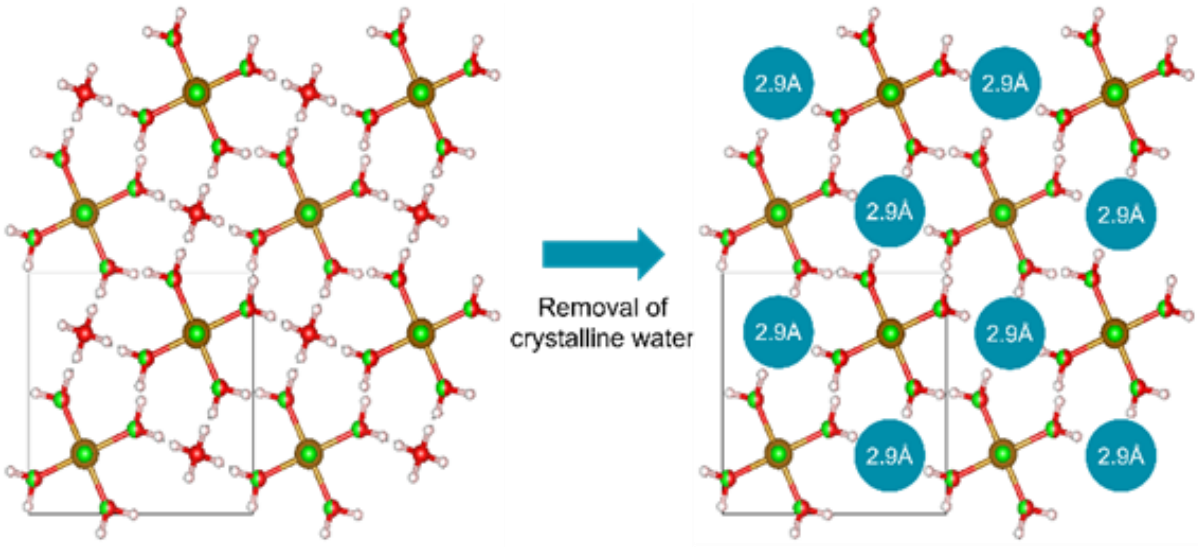

Fig 1. Schematic representation of b-$FeF_3.nH_2O$ structure.

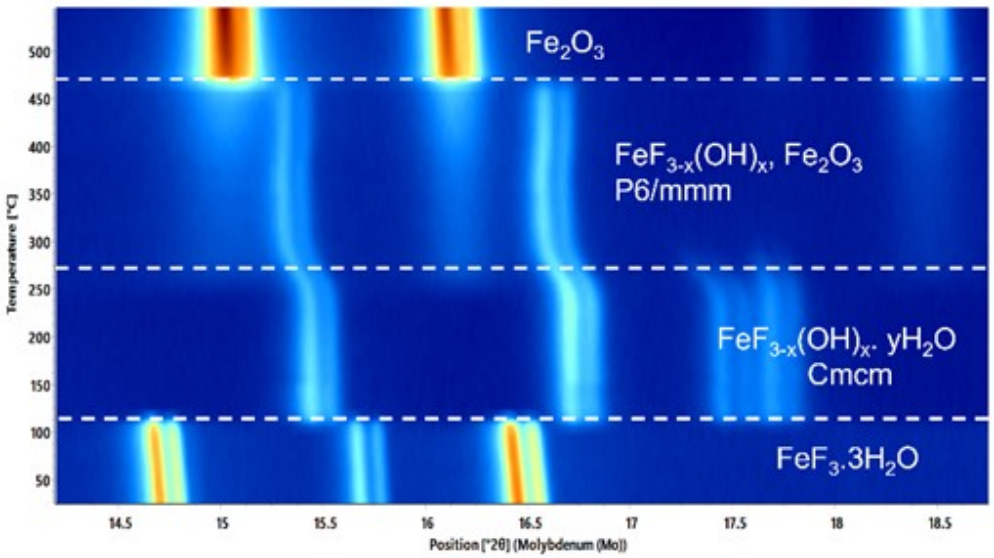

Figure 2. Set of XRD patterns collected from b-$FeF_3.3H_2O$, heated under self-generated atmosphere.

to the amount of the remaining crystalline water.

The structure, synthesis and properties of battery-relevant compositions of *b*-$FeF_3.nH_2O$ were extensively studied. Liu et al.[3] showed that $FeF_3.(1/3)H_2O$ composition with the hexagonal-tungsten-bronze (HTB) type structure[4] is the most promising for cathode application. Liu et al. also hinted that water does not only influence the conductivity of iron fluoride, but also stabilizes the HTB-type structure. A promising, cost-effective pathway to synthesize the HTB-type structure with $FeF_3.(1/3)H_2O$ composition was reported by Burbano et al.[5], where a partially controlled atmosphere (crucible wrapped in aluminium foil) was utilized. However, the synthetic route by Burbano et al. as well as the other reported synthetic pathways do not offer a mechanism for a precise control of water content, especially on the low concentration regime, which is the most interesting for battery applications.

We aimed to investigate in-situ the formation of $FeF_{3-x}(OH)_xnH_2O$ phases, to tune the crystal chemistry using a controlled atmosphere environment and to look for new phases not reported so far.

Methods

$FeF_3.3H_2O$ powder was placed in a capillary, one end of which was open to atmosphere. The capillary was placed inside an Anton Paar HTK1200N High-Temperature Oven-Chamber. In-situ high temperature hard radiation X-ray diffraction (XRD) measurements were performed on a Malvern Panalytical Empyrean diffractometer equipped with a Mo X-ray anode, focusing mirror and GaliPIX^{3D} detector. A Mo X-ray anode was utilized to ensure sufficient transmission through the sample as well as to extend the accessible range of d spacings. A series of 50 min scans in the 2Theta range between 4 and 50 °2Theta was collected in the temperature range from 25 to 550 °C. The HighScore suite[6] was used for the data representation and analysis.

Results and discussion

The temperature dependence of the in-situ heating of b-$FeF_3.3H_2O$ is shown in Figure 2. Here we are zooming on the narrow 2Theta range to highlight the observed phase transformations. The formation of previously reported $FeF_3.(1/3)H_2O$ with HTB-type structure is detected at ~ 130 °C. A series of $FeF_3.xH_2O$ compositions with varying wa-

ter content is followed up to ~ 260 °C, where the transition to the hexagonal $FeF_{3-x}(OH)_x$ occurs and Fe_2O_3 hematite starts to form. Finally, above 470 °C the entire sample is converted to hematite.

The aim of the case study is to understand whether it is possible to tune the water content of hydrated iron fluoride and to stabilize compositions with the crystalline water content y < 1/3. In Figure 3a we plot the water content of $FeF_{3-x}(OH)_x.yH_2O$ phase with HTB-type structure as a function of temperature. The first two data points at 140-150 °C correspond to the previously reported $FeF_3.(1/3)H_2O$ composition. However, at least nine more compositions with water content below 1/3 are observed. This observation suggests that it is not only possible to tune the amount of crystalline water in the structure, but also to achieve very low crystalline water content, down and beyond y = 0.125. This observation opens new possibilities to improve the electrochemical performance of hydrated iron fluoride.

The importance of crystalline water in stabilizing HTB-type structure of hydrated iron fluoride was suggested by Liu et al.[3], however, not confirmed experimentally. The in situ XRD data, presented here allow us to put forward the experimental evidence to this intuitive prediction. The geometrical difference between orthorhombic and hexagonal unit cells can be described by the orthorhombic distortion:

(1) $\sqrt{3} - {}^{b}/_{a}$

where *a* and *b* are unit cell parameters.

When the orthorhombic distortion is equal to zero, the orthorhombic unit cell can be described as hexagonal.

We fit the XRD data set in the range 130 – 360 °C using orthorhombic symmetry and calculated the orthorhombic distortion (1) as a function of temperature (Figure 3b). The large error bars of the data points falling in the stability field of P6/mmm phase are the result of fitting the hexagonal unit cell using orthorhombic symmetry. As seen in

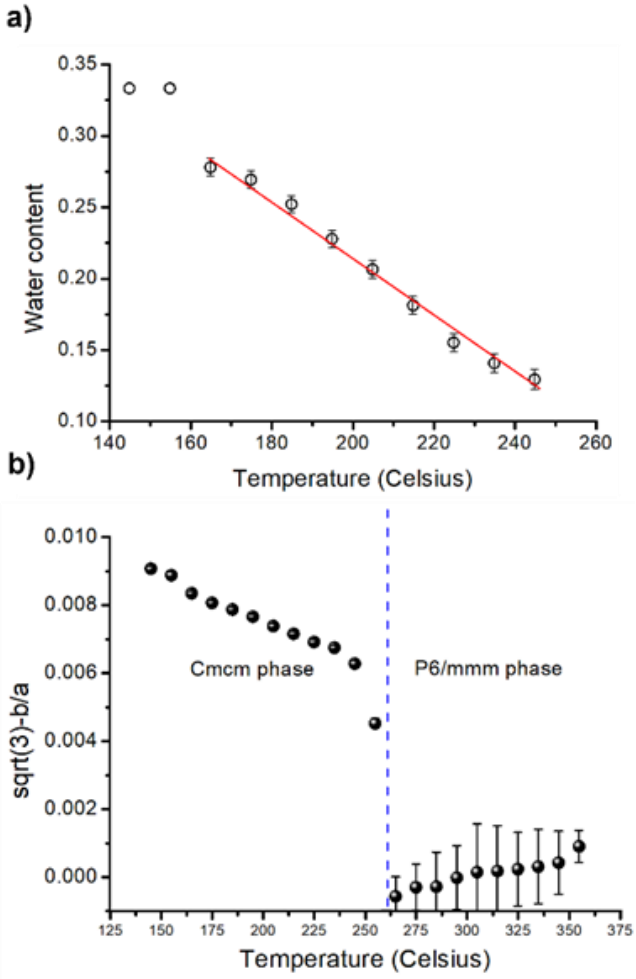

Fig 3. (a) Water content evolution in the FeF3-x (OH)x.yH2O series as a function of temperature; (b) orthorhombic distortion as a function of temperature.

Figure 3b the complete removal of crystalline water (~ 260 - 270 °C) results in the collapse of the structure and the transformation from orthorhombic to hexagonal symmetry. This observation experimentally confirms the importance of crystalline water in stabilizing the HTB-type structure of hydrated iron fluoride.

Conclusions

Heating of *b*-$FeF_3.nH_2O$ under self-generated atmosphere is followed by in situ hard radiation X-ray diffraction. The previously reported $FeF_3.(1/3)H_2$ with HTB-type structure[3,4] is synthesized above 130 °C. However, further temperature increase allows the stabilization of a series of $FeF_{3-x}(OH)_x.yH_2O$ compositions with water content, y, as low as

0.125. The ability to stabilize the tungsten bronze structure with y << 1/3 opens the possibility to improve the electrochemical capabilities of such an electrode as it offers more room for Li intercalation[3]. Furthermore, detailed in situ study of the dehydration of *b*-$FeF_3.nH_2O$ allowed us to confirm experimentally the intuitive prediction that crystalline water is responsible for the stabilization of the HTB-type structure of hydrated iron fluoride[3]. Finally, we demonstrate that a hard radiation crystallography with a self-generated atmosphere is an excellent tool to explore new chemistry for fluoride-based materials and stabilize new phases relevant for battery applications.

References

1. W. Kim, D. H. Seo, H. Gwon, J. Kim and K. Kang, "Fabrication of FeF3 nanoflowers on CNT branches and their application to high power lithium rechargeable batteries" Adv. Mater., **22 (46)**, 5260, (2010).
2. D. L. Ma, Z. Y. Cao, H. G. Wang, X. L. Huang, L. M. Wang and X. B. Zhang, "Three-dimensionally ordered macroporous FeF_3 and its *in situ* homogenous polymerization coating for high energy and power density lithium ion batteries" Energy Environ. Sci., **5**, 8538, (2012).
3. L. Liu, H. Guo, M. Zhou, Q. Wei, Z. Yang, H. Shu, X. Yang, J. Tan, Z. Yan, X. Wang "A comparison among $FeF_3{\cdot}3H_2O$, $FeF_3{\cdot}0.33H_2O$ and FeF_3 cathode materials for lithium ion batteries: Structural, electrochemical, and mechanism studies" J. Power Sources, **238**, 501 (2013).
4. M. Leblanc, G. Ferey, P. Chevallier, Y. Calage, R. J. De Pape "Hexagonal tungsten bronze-type FeIII fluoride: (H2O)0.33FeF3; crystal structure, magnetic properties, dehydration to a new form of iron trifluoride " Solid State Chem., 47, 53 (1983).
5. M. Burbano, M. Duttine, O. Borkiewicz, A. Wattiaux, A. Demourgues, M. Salanne, H. Groult and D. Dambournet, "Anionic Ordering and Thermal Properties of $FeF_3{\cdot}3H_2O$" Inorg. Chem., 54(19), 9619 (2015).
6. T. Degen, M. Sadki, E. Bron, U. König, G. Nénert, "The HighScore suite" Powder Diffraction, **29 (S2)**, S13 (2014).

Laboratory Based X-Ray Microscopy

D. B. Fox[1 *], S. R. Kada[1, 2], J. Zhang[1, 2], J. Wang[2], S. Mayo[1], A. Sola[1], A. Trinchi[1], J. Jacob[1], J. Razal[2], M. R. Barnett[2], N. Wright[1], P. A. Lynch[1, 2]

[1]*Commonwealth Scientific and Industrial Research Organisation, Clayton, 3168. Australia.*

[2]*Institute for Frontier Materials. Deakin University. 75 Pigdons Road, Waurn Ponds, Victoria, 3216. Australia.*

* Corresponding author: David.Fox@csiro.au

Abstract

Here we report on a new laboratory based X-ray facility for X-ray microscopy and dynamic materials testing. Based on a dual port, high brightness Excillum Metal Jet X-ray source, beamline I offers fully automated SAXS-WAXS capabilities while beamline II is modular to enable rapid switching from polychromatic diffraction to micro-computer tomography (MicroCT). The attributes of the new facility are highlighted by 3 case studies. The first case study demonstrates correlation microscopy at different length scales- microCT is used to assess macro-scale porosity in $T_3C_2T_x$ MXene, while SAXS-WAXS is used to interrogate channel alignment and porosity at the nm level. Case study 2 addresses the role of boron nitride sheets as a grain size refinement approach for additive manufacturing of Ti alloys. Finally, in-situ observation of plasticity onset in lightweight Mg alloys is presented.

Introduction- InSitX

InSitX represents an exciting new joint program between Deakin University and CSIRO for the development of new *in-situ* and correlative X-ray microscopy experiments. The facility aims to lead in the development of new science that is both interestingly unique internationally which delivers impact for advanced manufacturing priority areas. InSitX is a world first X-ray facility with near synchrotron capabilities. By application of a dual port Excillum Metal Jet X-ray source, the facility houses two beamlines (Figure 1),

Fig 1. InSitX dual beamline X-ray microscopy facility.

Beamline I is a turn-key Xenocs Xeuss 3.0 SAXS-WAXS system, operating at a fixed energy of 9.2keV with a range of resolution settings, either high flux or ultra-high resolution (beam size to 150 x 150 µm). The entire system can be run in vacuum with the SAXS-WAXS data captured by automated translation of the detector from 20cm (WAXS) up to 1800cm (SAXS).

Beamline II is a custom modular system built in-house, enabling spatially resolved polychromatic diffraction and MicroCT.

Case Study I:

$T_3C_2T_x$ MXene is a new 2D material, regarded as a promising candidate for supercapacitors and batteries due to its high electrical conductivity and volumetric capacitance. MXene foam fabrication, based on freeze casting methods, is an effective approach to tailor the microstructure of MXene channels within these foams. For freeze casting, the size of ice crystals defines the pore sizes while the ice growth direction dictates channel orientation. In general, the porous structure of MXene

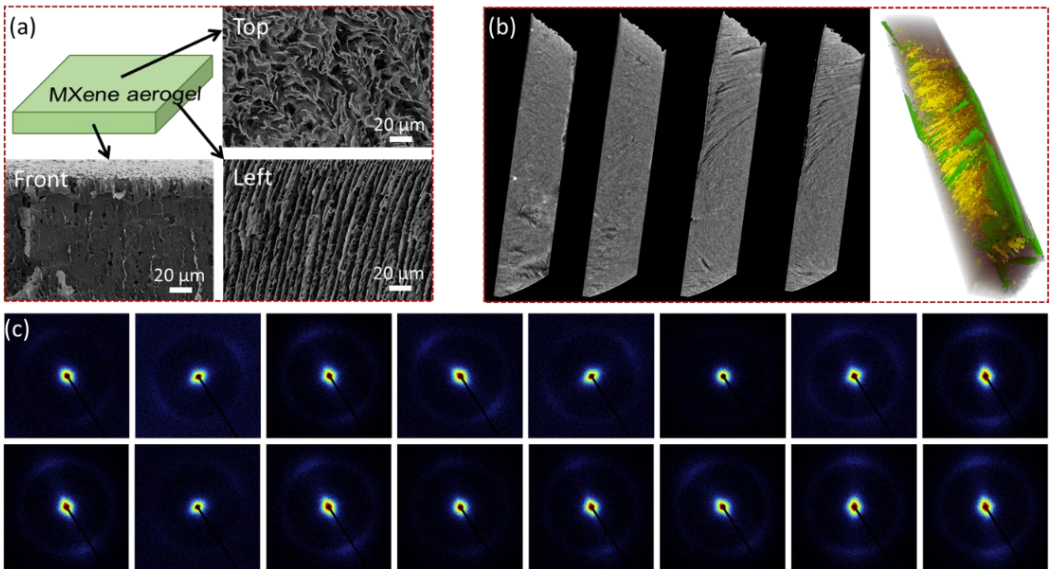

Fig 2. Summary of 2D MXene microstructure. (a). Schematic illustration of the MXene aerogel and microstructure as observed by SEM. (b). MicroCT reconstruction of the MXene porous microstructure. (c). High resolution SAXS-WAXS mapping over the same region studied by MicroCT.

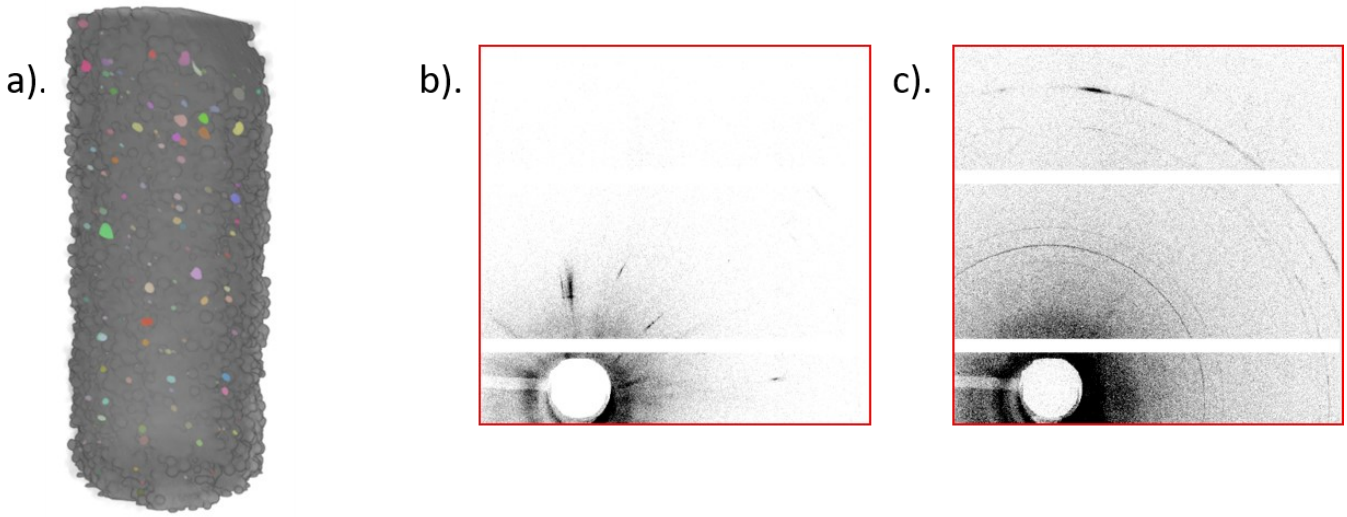

Fig 3. Summary of X-ray data acquired for the additive manufactured Ti pillars. (a). MicroCT reconstruction of the CP-Ti pillar. (b). Diffraction data from the CP-Ti pillar. (c). Diffraction data from the Ti-BN pillar.

aerogels can be characterized using scanning electron microscopy (SEM) by looking at the broken profile of aerogels, as shown in Figure 2a. However, the inner channel structures cannot be readily observed. Herein, the unique combination of Micro-CT and SAXS/WAXS is utilised to study the interior porous structures and channel alignment, respectively.

The reconstructed MicroCT data in Figure 2b shows the dispersion of the porous structure throughout the interior of MXene aerogel (greyscale reconstruction) with a thickness of 250 µm. Note the colour reconstruction is used to visualise the interior *vs.* surface porous network, yellow interior and green surface, respectively. To observe MXene stacking and alignment, SAXS-WAXS mapping (Figure 2c) was undertaken. In our previous study on highly aligned MXene films, we found that when the plane of 2D MXene flakes is parallel to the incident X-ray beam the (002) peak formed pronounced preferred orientation. In contrast, here we observe only a slight degree of preferred orientation, *i.e.* the patterns appear more isotropic in nature. In the future we plan to use this approach as a tool to optimise MXene aerogel performance by quantitative analysis of the layer spacing, packing density according to ice growth direction.

Case Study II: Application of Boron Nitride sheets in Additive Manufacturing:

One approach for controlling columnar grain size in laser-based powder bed fusion additive manufacturing is by the addition of boron nitride nanosheets during the build process. Here we utilize both MicroCT and polychromatic diffraction to study the effect of the additive manufacturing process on the grain size in small pillars of commercially pure titanium samples made with (Ti-BN) and without (cp-Ti) boron nitride. Figure 3 provides a summary of the data acquired for each sample. For both samples, the void density was similar. An illustration of the void size and density is shown for the cp-TI sample in Figure.3a.

Spatially resolved polychromatic diffraction offers a single-shot, rapid tool for grain size measurement. By application of an energy bandpass, rather than a monochromatic source of X-rays, the observed form of diffraction data is dependent on the incident probe size. When the grain size is << probe size a diffraction ring is observed. On the other hand, when the grain size is >= to the probe size, Laue patterns from individual grains can be observed. In this case, the cp-Ti sample did show an increased grain size, as evidenced by the observation of Laue patterns shown in Fig. 3b. Conversely, for the sample treated with BN a smaller

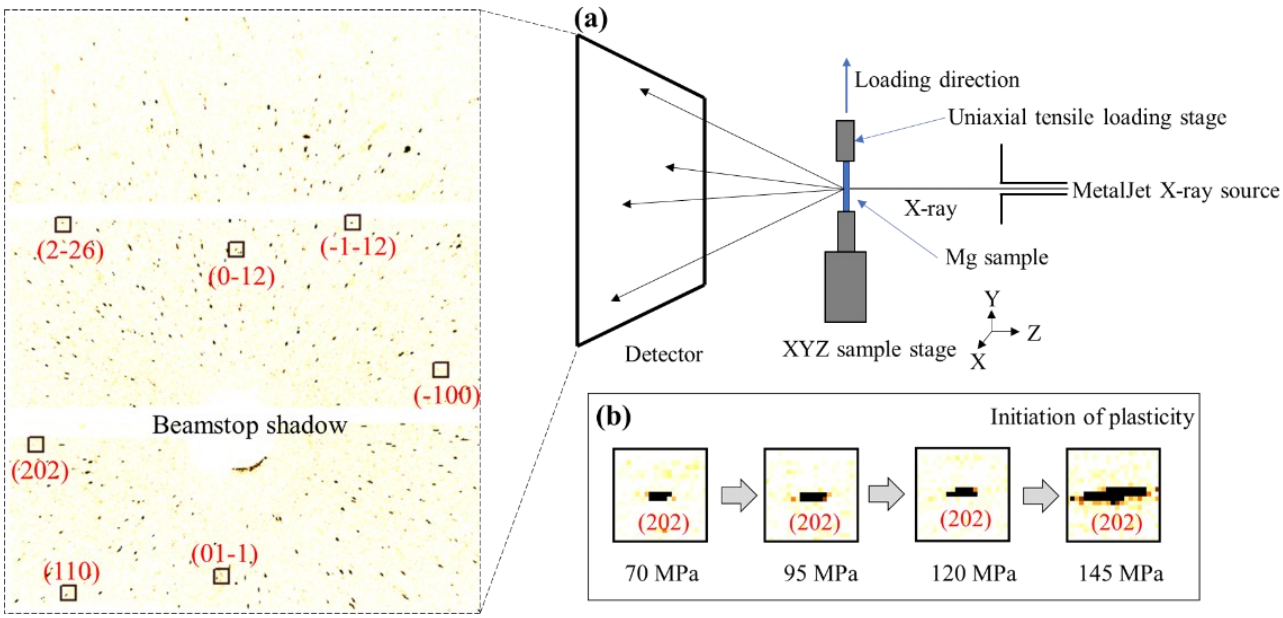

Fig 4. (a) Schematic illustration of the in-situ loading experiment as conducted on beamline II. The inset shows a typical Laue data. An indexed Laue pattern belonging to a particular individual grain are noted using (hkl) Miller indices. (b) Example illustrating how the (202) reflection of the indexed grain evolves with the increased load.

grain size is identified by the complete and spotty ring pattern shown in Figure. 3c.

Case Study III: In-situ observation of plasticity onset in lightweight metals alloys

In-situ observation of plasticity onset in lightweight metals and alloys hereby is demonstrated, for a lightweight Mg alloy (95.5wt.% Mg and 4.5wt.% Zn). Figure 4 (a) shows the set-up of the main components for the in-situ loading experiment. An aperture of 50 micron is used to control the polychromatic X-ray beam size. A raster scan approach is adopted to map individual grains from the middle of the gauge section out as the applied load is increased incrementally. The inset in Figure 4 (a) is a typical Laue map obtained from the 70 MPa load step. In this map, seven Laue spots are highlighted by rectangular boxes, and based on pattern indexation were shown to belong to the same individual grain. To highlight, Figure 4 (b) shows the evolution of one of these reflections during loading. There is an obvious broadening for this (202) reflection at 145 MPa – which indicates the onset of plasticity.

The rich information obtained from processing the acquired polychromatic diffraction Laue data also includes the orientation matrix and strain tensor of individual grains in a bulk polycrystalline material. By combining the above information of the individual grains at different loads and the knowledge of the available slip modes in the studied alloy systems, the activation of a particular slip mode and its critical resolved shear stress (CRSS) at the onset of plasticity can be largely determined. Finally, the capability to quantify individual grain structure information from a laboratory instrument is highly useful if further high-resolution/ high speed X-ray studies are to be performed at a Synchrotron facility.

Conclusion

By application of a high brightness liquid metal jet X-ray source, near synchrotron like X-ray microscopy studies have been realized in a laboratory setting. One of the one of the key benefits of the laboratory based system, is the potential for immediate instrumental access which is not possible with the equivalent synchrotron based experiment. It is foreseen, upon further system optimization in terms of spatial resolution and dwell time speed, a broader range of applications will be possible.

A new round of the SAAFE Internship Program is now open!

Open to PhD students or Postdocs in nuclear science or engineering (from Australia OR New Zealand) interested in travelling to France for their research project

See full criteria and apply now at https://ainse.edu.au/saafe/.

Awards and Grants

Malvern Panalytical Young Scientist Award (submit your entry by September 30 2022)

Calling all young scientists under 35 years!

Share your published paper where data collected was from Malvern Panalytical equipment

Published 1st Jul 20 - and 31st Dec 21

Recognized journal with Impact Factor >2.5

Stand to win €5,000

More information here:

https://www.malvernpanalytical.com/en/campaigns/scientific-awards

Awards and Grants

a

Support of research communities has many facets, but all of them aim to encourage scientific exchange, continuous learning and collaborations. One of them is the DECTRIS award, which supports innovative researchers to share their findings.

This year's DECTRIS award went to Dr. Li Na, beamline scientist and group leader at the Shanghai Synchrotron Radiation Facility, for her work on Small Angle Scattering (SAS) methodologies and their applications to biological materials. Congratulations!

How about supporting less-privileged researchers? Andreas Förster Grant might be the answer! The grant will be launched

2022 SPECTRA^{plus} School - Australia & New Zealand

Our SPECTRA^{plus} School Australia & New Zealand is scheduled to take place on 17-21 October 2022 (Mon-Fri), 9AM – 5 PM at our training facilities in Preston. This hands-on course is an introduction to SPECTRA^{plus} Version 3/4 for WDXRF systems, and will cover alignment, calibration and maintenance.

There are both in person and virtual options available. To facilitate interaction between participants and trainers, limited seats are available on a first-come-first-serve basis.

Find out more here: https://www.bruker.com/en/services/training/elemental-analyzers/application-trainings/spectraplus-school-aunz.html

Featured Training Courses

Malvern Panalytical training courses

- XRF in the workplace - AUD 4,200 excluding GST (Early bird closes 2 mths prior: AUD3,700)
  - Nov 2022: https://www.malvernpanalytical.com/en/learn/events-and-training/webinars/W221114-XRF-Workplace.html
- SuperQ WDXRF software training for Malvern Panalytical's Zetium and Axios users - AUD 2,500 excluding GST
  - Oct 2022: https://www.malvernpanalytical.com/en/learn/events-and-training/webinars/W221011-SuperQ-XRF-Training.html

FREE 1 year XRD license for professors
(up to 3 trial licenses per university department)

- HighScore Plus version 5.1 (latest version) for powder XRD analysis
- AMASS software (new) for thin films research
- Request for your license here
- Check find useful webinars on how to apply the software for your XRD analysis, all available via the same link.

Malvern Panalytical
a spectris company

Live webinars (Register for the recording):

17 Aug Augment your battery research with dedicated non-ambient in-operando XRD: https://www.malvernpanalytical.com/en/learn/events-and-training/webinars/W220814-Plugvolt-XRD

15 Sep Ask an Expert! Hints and tips for customizing your thin film analysis using XRD: https://www.malvernpanalytical.com/en/learn/events-and-training/webinars/W220915AMAskanExpertXRD

(Webinar on demand) Check for microstructural defects in additive manufacturing using XRD https://www.malvernpanalytical.com/en/learn/events-and-training/webinars/W20220526AMXRD

Custom made X-ray shielding enclosures for Science and Industry

Enclosures can be designed around a specific source and/or detector and are fully interlocked and supplied with fail-safe warning lamps.

Shielding specified for 70 kV with 8 x HVL attenuation. Mounted on an Optical bench and used with a high brilliance source. Steel frame with removable steel panels and doors with Lead lining and Lead glass and Aluminium trim panels.

Interior view of a multi-door enclosure also for Mounting on an Optical bench.

Heavy duty enclosure for vertical source application. Could be mounted on casters for mobility.

Contact Rod Clapp at Diffraction Technology to discuss your requirement and for a budget quote. www.diffraction.com.au e-mail diffraction@bigpond.com, phone 03 9787 3801

ROWE SCIENTIFIC PTY LTD www.rowe.com.au

For accuracy and professionalism

Providing laboratory supplies to the scientific community across Australia since 1987.

We are proudly a 100% Australian owned company.

Quality System
Quality Endorsed Company
ISO 9001:2015
LIC 10372
SAI Global

XRF - XRD Sample Preparation

Rowe Scientific are now exclusively supplying the SOMAR brand of Australian made XRF pellet cups.

We have purchased the assets of SOMAR Australia and incorporated their pellet cup manufacturing into our Perth Facility.

XRF Liquid Cups

FREE SAMPLES
CONTACT US TODAY

These cups allow the analysis of solutions by XRF, and fit all common makes of XRF instruments, including X-Unique II, PW2400, PW2404, Axios, and many PANalytical instruments.

- Free trial samples available
- Very cost competitive.
- Avoids cross contamination between samples - cups are disposable.
- Made from polypropylene - chemically inert.
- Packaged under clean room conditions - free from silica and other airborne particulates.

For ordering information, download the XRF - XRD brochure by visiting our website

www.rowe.com.au

To find out more or to acquire your FREE samples, call your local Rowe Scientific Pty Ltd office

SCAN TO DOWNLOAD XRF-XRD BROCHURE

https://goo.gl/1kCVUw

ROWE SCIENTIFIC PTY. LTD. www.rowe.com.au

South Australia & NT
Ph: (08) 8186 0523
rowesa@rowe.com.au

Queensland
Ph: (07) 3376 9411
roweqld@rowe.com.au

Victoria & Tasmania
Ph: (03) 9701 7077
rowevic@rowe.com.au

Western Australia
Ph: (08) 9302 1911
rowewa@rowe.com.au

New South Wales
Ph: (02) 9603 1205
rowensw@rowe.com.au

Quality System
Quality Endorsed Company
ISO 9001:2015
LIC 10372
SAI Global

AXAA Website and Contacts

Please visit our website, www.axaa.org, for further information, or follow us on Twitter @axaa_org.

NATIONAL COUNCIL PRESIDENT:

Jessica Hamilton
Australian Synchrotron (ANSTO),
800 Blackburn Road,
Clayton, VIC 3168
Telephone: (03) 8540 4297
e-mail: hamiltoj@ansto.gov.au

NATIONAL COUNCIL VICE PRESIDENT:

Nathan Webster
CSIRO Mineral Resources, Box 10
Clayton South, VIC 3169
Telephone: (03) 9545 8635
e-mail: nathan.webster@csiro.au

NATIONAL COUNCIL SECRETARY:

Anita D'Angelo
Australian Synchrotron (ANSTO),
800 Blackburn Road,
Clayton, VIC 3168
Telephone: (03) 8540 5397
e-mail: anitad@ansto.gov.au

NATIONAL COUNCIL TREASURER:

Sally Birch
CSIRO Mineral Resources, Locked Bag 2
Glen Osmond, SA 5064
Telephone: (08) 8303 8487
e-mail: sally.birch@csiro.au

NATIONAL COUNCIL COMMUNICATIONS EDITOR:

Valerie Mitchell
Australian Synchrotron (ANSTO),
800 Blackburn Road
Clayton, VIC 3168
Telephone: (03) 8540 4297
e-mail: mitchelv@ansto.gov.au

NATIONAL COUNCIL MEMBERS:

Matthew Rowles (Curtin, WA)
Brianna Ganly (CSIRO, NSW)
Daniel Fanna (WestSyd, NSW)

AXAA Membership

All registered participants of the AXAA-2017 conference are automatically granted AXAA membership for 3 years. Alternatively, new memberships can be obtained free of charge, by making an application to the National Council.

Candidates should send the membership form from the AXAA website, and a short statement about how they intend to contribute to the organisation, to the National Council Secretary Anita D'Angelo.

AXAA Resource Centre

There are a range of resources available on the AXAA website, including video recordings of the two Public Lectures at AXAA-2017, tips for Rietveld Analysis, Clay Analysis, XRF tips, and more. We welcome further contributions to our Resource Centre.

Next AXAA Newsletter

The next issue of the AXAA Newsletter will be distributed in December 2022. Please feel free to send contributions for the newsletter to Valerie Mitchell at *ausxray@gmail.com*. Any comments or feedback about the Newsletter are welcome.

A Day in the Life of an X-ray / Neutron Scientist

We are seeking posts for our 'Day in the Life' series. If you'd like to contribute, or know someone who might be interested, please contact National Council